Proceedings World Geothermal Congress 2020+1
Reykjavik, Iceland, April - October 2021

Feasibility Assessment of Hydraulic Fracture Stimulation Treatment in the Wayang Windu Geothermal Field (West Java, Indonesia)

F. Pizzocolo*, Mulyadi***, B. Bratakusuma***, J.H. ter Heege**, P.A. Fokker**

* TNO – Materials Solutions, Eindhoven (NLD)

** TNO – Applied Geoscience, Utrecht (NLD)

*** Star Energy, Jakarta (IDN)

francesco.pizzocolo@tno.nl

Keywords: thermo-hydro-mechanics coupled model, poroelasticity, stimulation

ABSTRACT

After years of exploiting steam, geothermal wells may need stimulation to remain economically profitable. In some cases, hydraulic fracturing can be a suitable technique to improve steam production or to create new geothermal pay zones. Performing such a treatment in a geothermal volcanic environment presents several challenges. We investigated technical and geological issues that might affect the effectiveness and efficiency of stimulation, focusing on the feasibility of hydraulic fracturing in the Wayang Windu geothermal field (West Java, Indonesia). A major issue is given by the way in which the wells of this field are completed: a long perforated liner in an open hole section. When isolation of a short section of the perforated liner is not technically possible, or is economically too expensive, hydraulic fracturing might not be the proper stimulation technique. Moreover, executing a hydraulic fracture treatment on the long perforated intervals (500-1500 m) typical of the wells of the Wayang Windu field might jeopardize the integrity of the well.

1. INTRODUCTION

Reducing CO_2 emissions is greatly helped by geothermal energy. Even though geothermal power plants have lower efficiency in generating electricity than other large scale energy technologies, such as coal, gas, oil and nuclear, their virtually zero emission rates in combination with the possibility of providing stable energy supply make geothermal energy attractive. In addition, while other green energy sources as solar or wind suffer from fluctuating supply, geothermal energy can be used as a base load.

A very high geothermal potential is found in Indonesia, located along the so called “ring of fire”. This allowed the Indonesian Geothermal Energy company Star Energy to become one of the world leaders in development and exploitation of this renewable energy. The scale of operations also allows the development of optimal production strategies. Among others, they require the investigation of stimulation options in case a well is underproducing or production is declining. Such options entail conventional stimulation techniques as thermal and acid stimulation, but also hydraulic fracturing.

Hydraulic fracture treatments in conventional oil and gas fields target pay zones: rock layers in which fossil fuels are present in exploitable quantities. These target zones are usually isolated with packers to rightly pinpoint the fracture growth. In a geothermal system, the goal is to stimulate the zone around a well that is underperforming by connecting pre-existing fractures or by creating new pathways for the steam through the initiation and propagation of new fractures. Historically, the first hydraulic fracturing stimulation, with an injection of approximately 21000 m^3 of water at 3.5 km of depth, was performed in the Fenton Hill field (New Mexico) in 1970 (Rachmat, 2015). In the past decades this treatment was applied in various fields (East Mesa, Baca, Raft River, Salak, Soultz-Sous-Foretz, Landau and Wayang Windu) with different degrees of effectiveness.

Target zones in geothermal wells can often not be isolated due to the completion design. Many wells are completed with a perforated liner in a long open-hole section. Such completion poses a number of challenges for hydraulic stimulation. Firstly, it requires large volumes of fracture fluids and proppant, affecting the economic feasibility of the stimulation. The required volumes are even further increased when the field exhibits a natural fracture network, because a high percentage of the injected fluids will penetrate the formation instead of creating induced fracture volume. Further, because of the stress profile, an induced fracture is expected to develop preferentially around the top of the perforated liner: the fracture location can thus not be optimized. And finally, there is a risk of jeopardizing the wellbore integrity because of the absence of a cemented annulus.

We have investigated the feasibility of applying a hydraulic fracture stimulation to the Wayang Windu field (West Java, Indonesia). We particularly address the challenge of the long sections of the wells connected to the reservoir in combination with the high leakoff values expected, and the wellbore integrity issues resulting from the large stress anisotropy and open-hole completions.

2. BACKGROUND

2.1 Characteristics of the Wayang Windu field

A comprehensive overview of the geology, fracture system and operational development of the Wayang Windu field can be found in the works of Bogie et al (2008), Fauzi et al (2015) and Masri et al (2015); further data were made available by Star Energy in their geology reports. We here summarize the key features and the data relevant for the present study.

Wayang Windu is located approximately 30 km south of the city of Bandung in West Java (Indonesia) and is considered one of the most efficient geothermal fields of the world. It is the largest one in Indonesia, with 25 wells (22 production and 3 injection wells). The field produces steam at temperatures up to 300°C.

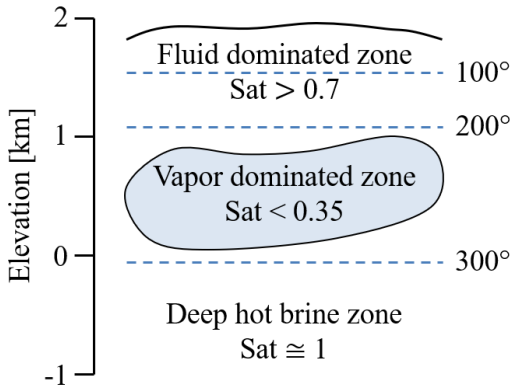

Figure 1. Simplified temperature and fluid saturation profiles along depth of the Wayang Windu geothermal field. Sat = fluid saturation.

The reservoir fluids are accumulated in the pores and fractures of volcanic rocks; flow is facilitated by a very dense fracture network. The field is generally interpreted to be a transitional geothermal system between vapor-dominated and liquid-dominated conditions. The pore pressure profile can consequently be divided into three subdomains (Figure 1): a liquid-dominated hydrostatic zone above the reservoir, a two-phase vapor-dominated steam zone in the reservoir and a liquid saturated brine zone below the reservoir. A transition zone with a thickness that varies from 50 to 200 meters is present between the overburden and the reservoir. The top of the reservoir is placed where the temperature profile becomes approximately constant. The contact surface between water and steam is assumed to lie at, or near, the top of reservoir.

The Wayang Windu field is a densely fractured system. The feasibility and optimization of hydraulic fracturing of such a system critically depends on data of the mechanical stress and the fracture network. Near-well stress orientations were taken from the calculations using borehole breakouts by Masri et al (2015). The local stress field is often not consistent with the regional tectonics because of the geological conditions of volcanic environments: a least principal stress at 310° in a transitional state from normal to strike-slip regime. Masri et al (2015) further employed 1D and 3D geomechanical analyses to calculate the gradients of the in-situ stresses. We used the average values and considered them constant through all rock's formations and lithology (Table 1).

Masri et al (2015) determined fracture densities (D_{frac}, the measured number of fractures per meter) based on measurements in 16 wells. The numbers vary from 0.6 m^{-1}, in breccia with porosity 6-8 %, to almost 2.5 m^{-1}, in lava with porosity 0-4 % (Masri et al, 2015). For the average porosity in the steam zone of the geothermal reservoir (15 %), the Breccia has an average fracture density of 0.8 m^{-1}, the Tuff-Breccia has 1.3 m^{-1}, the Lapilli-Tuff 1.4 m^{-1} and the Tuff 0.9 m^{-1}. The average density of the different facies is 1.1 m^{-1}, while the average value for the Wayang Windu field is approximately 1.5 m^{-1}. In spite of the large amount of more than 9000 detected fractures, the fluid flow depends on just a limited amount of clusters with a densely interconnected system. Those structures have a semi-regular spacing of 70 meters, with a different predominant flow direction for each lithology. Those structures must be connected to the well to achieve a successful stimulation.

The major faults in West Java form a conjugate pair of strike-slip system (NNW and NE) consistent with the regional compression state due to near perpendicular (> 80°) subduction. The mechanical properties collected during field and laboratory measurements are listed in Tables 2 and 3 (Bogie et al, 2008). Elastic moduli are averaged for the overburden and the reservoir.

Table 1. In situ stress gradients.

Gradient σ_V	24	kPa/m
Gradient $\sigma_{h,max}$	26	kPa/m
Gradient $\sigma_{h,min}$	13	kPa/m

Table 2. Mechanical properties of the different facies that are found in the Wayang Windu field. C_0 = uniaxial compressive strength. β = failure angle. T_0 = tensile strength. E = Young's modulus. ν = poisson ratio.

Rock's facies	Density	C_0	β	T_0	E	V
	[g/cm³]	[MPa]	[°]	[MPa]	[GPa]	[-]
Tuff breccia	2.55	10,77	47	0,11	7.5	0.23
Lava	2.72	13,79	44.7	0,1	10	0.18
Tuff	2.35	3,77	52.3	0,13	8	0.15
Lapilli tuff	2.4	10,14	45.3	0,1	8	0.23

Table 3. Rock mechanical properties.

Zone	TVD at bottom	Young's modulus	Poisson ratio	Fracture toughness
	[m]	[GPa]	[-]	[bar * $m^{1/2}$]
Overburden	910	7.5	0.23	3
Reservoir	1600	8	0.23	3

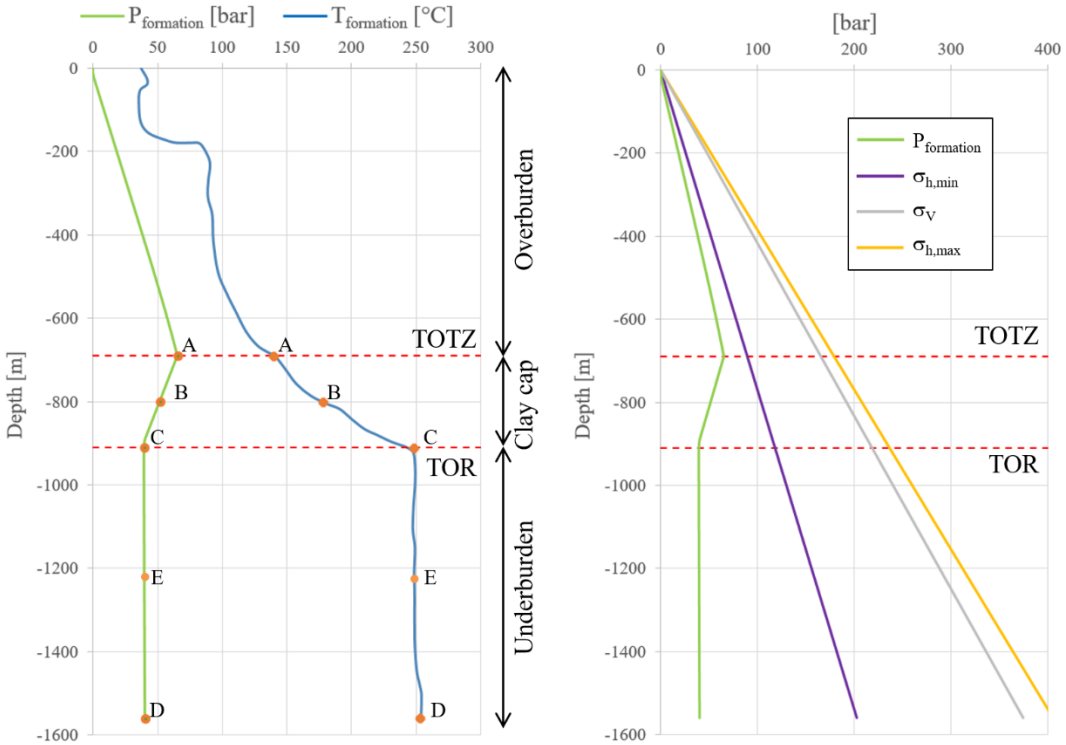

Figure 2. TOTZ = top of transition zone. TOR = top of reservoir. Left: temperature and pressure profiles along depth (TVD). The magnitude of pressures in points A, C and D was directly measured. The pore pressure profile between points A and C is an interpretation. Right: pressure and in situ stresses profiles along depth (TVD).

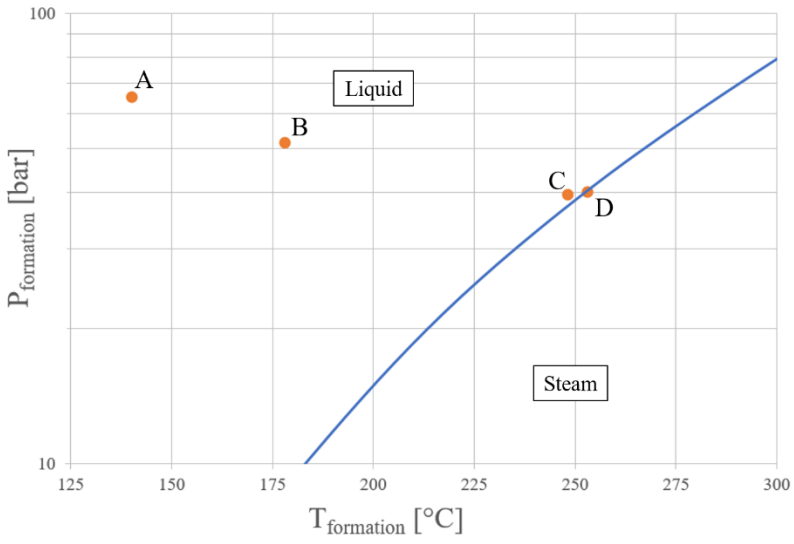

Figure 3. Water phase diagram around the pressure and temperature values of the transition zone and dry steam reservoir. A = top of the transition zone, B = center of the transition zone, C = top of the reservoir (base of the transition zone), D = total depth of the case study well.

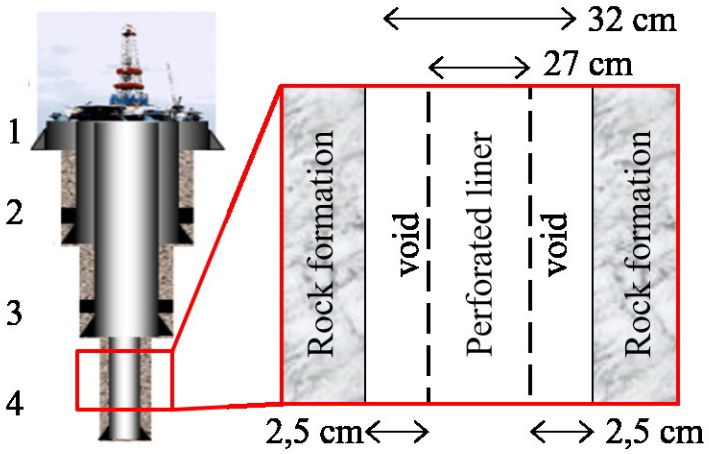

Figure 4. Typical profile of a geothermal well in the Wayang Windu field. The profile is divided into 4 sections (Table 4). 1: vertical cemented section. 2 and 3: deviated cemented section. 4: not-cemented deviated section, completed with a perforated liner that is not in contact with the wellbore walls. In this reference case the void annulus between casing and rock formation has an average thickness of 2,5 cm.

Table 4. Casing summary of the well.

Section	Hole Diameter	Depth		Casing shoe diameter	Cement
	[cm]	mMD [m]	TVD [m]	[cm]	
1	76	48	343	66	Yes
2	66	403	402.5	51	Yes
3	45	890	817.8	34	Yes
4	32	1600	1279.7	27	No

Our simulations used the temperature profile represented in Figure 2. The profile was based on measurements during a completion test – except above the top of the reservoir, where an interpretation based on Star Energy's conceptual model was used. For that section, temperature measurements could not be used because a heating-up process occurred while running the completion tests. Figure 2 also represents the pore pressure profile. In the transition zone between fluid and dry steam phase (between points A and C) an underpressure gradient is present. This is generated by an impermeable clay cap acting as hydraulic barrier, which is typical for geothermal reservoirs in volcanic enviroments (Cumming, 2009). The combination of pressures and temperatures on the depths indicated in Figure 2 are also shown in the water phase diagram (Figure 3). In the transition zone (points A and B) the water is in the liquid phase. At the top of the reservoir (point C) the water basically reaches the steam phase. The pressures of the overburden and of the steam zone were measured directly, while the pressure profile within the transition zone is an interpretation of the pore pressure behavior.

Simulations of hydraulic fracturing finally require input for reservoir porosity and permeability, reservoir fluid viscosity, and spurt loss. The permeability of the rock mass is low, 0.001 mD, and the porosity is 15%. Viscosities were assigned on the basis of standard thermodynamic correlations for the average temperature, pressure, and phase in the different zones. An overview of the fluid loss data is given in Table 5. The mean formation temperature that was considered was 250°C and the injected fluid inlet temperature was 30°C.

Table 5. Fluid loss data. The spurt loss is the fluid volume loss of fluid per unit area of fracture face that happens immediately after the beginning of the hydraulic fracture stimulation and it is calculated by the numerical simulator (Meyer, 2016). * = permeability of the unfractured rock matrix.

Zone	TVD at bottom	Porosity	Viscosity	Permeability*	Spurt Loss
	[m]	[%]	[mPa·S]	[mD]	[cm]
Hydrostatic	690	15	0.28	0.001	0
Transition	910	15	0.15	0.001	0.306
Steam	1600	15	0.013	0.001	0.611

The length of the non-cemented section in the Wayang Windu wells varies between 400 and 1500 meter. The base section is typically completed with a perforated liner, production is accomplished without tubing. Our study focuses on the stimulation of a typical dry-steam well of the Wayang Windu geothermal field (Figure 4, Table 4). This type of steam contains less than 1% of moisture.

2.2 Hydraulic stimulation of geothermal fields

Several stimulation techniques can be applied when the production of a geothermal well is uneconomic. In the Wayang Windu field, the fluids mainly flow through the faults and fractures. In such a situation, hydraulic stimulation can either activate and stimulate the already existing network of fractures by fault reactivation, or it can create new pathways by tensile fracturing. The feasibility of different types of hydraulic fracture stimulation depends on the stress situation (Figure 5). A correct estimation of the in situ stress state of the subsurface and the fracture system is therefore essential to assess which stimulation technique has the highest success potential. Such a geomechanical study should ideally be performed before drilling a well, to locate "sweet" spots (sections of the reservoir where profitable steam flow can be achieved with little or no stimulation) and to optimize the well trajectory.

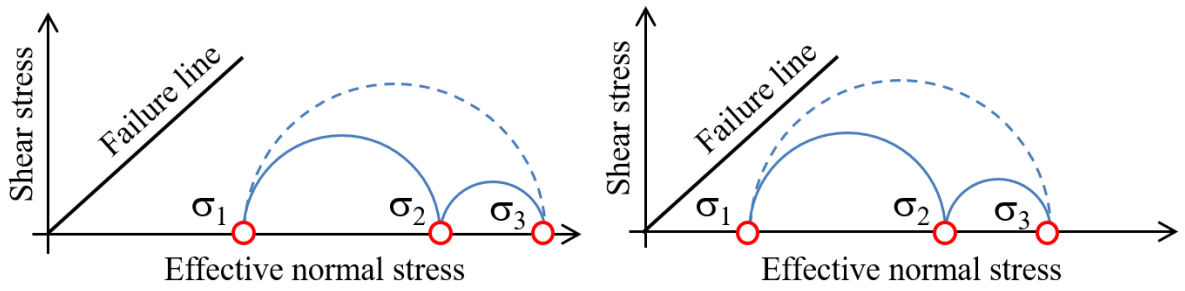

Figure 5. 3D Mohr – Coulomb representation of the state of stress of a fracture. In the Wayang Windu field, σ_2 is the vertical in situ stress (σ_v). σ_1 is the minimum in situ stress ($\sigma_{h,min}$), σ_3 is the maximum in situ stress ($\sigma_{h,max}$). Left: the fracture is "far" from the failure state. To reach failure, a hard stimulation (such as large injection rates and pressures) might be necessary. Right: if a fracture is closer to failure, a soft stimulation might be enough to improve the production via reactivation of existing fractures.

A hard stimulation approach, such as a hydraulic fracture treatment (Figure 6), can be required for several reasons: to overcome near wellbore damage, to create new tensile fractures around the well or to shear a cluster of fractures that are too far from a failure state.

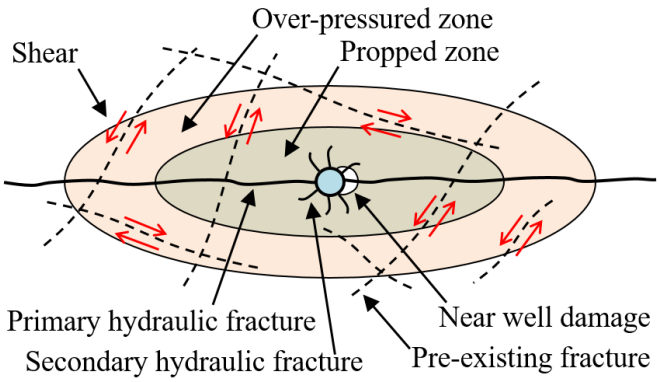

Figure 6. Top view of the stimulated area around a well after a hydraulic fracture treatment is performed. Such a treatment can propagate long tensile fractures in the direction of $\sigma_{h,max}$ and short fractures in the direction of $\sigma_{h,min}$. Moreover, proppant can flow into the pre-existing fracture that are present in the propped zone and the fractures that are located into the extended over-pressured zone might undergo hydroshearing (modified after Dusseault et al, 2011).

Hydraulic stimulation involves the pumping of fluid into a propagating fracture under high pressures. Part of the fluid does not remain in the fracture but is lost to the reservoir – this is called the fluid leakoff. It is driven by the pressure difference between injected fluid in the fracture and pore fluid in the reservoir, and by the resistance resulting from the reservoir permeability and the fracture network. The fluid leakoff is the principal factor controlling the induced fracture dimensions – height, length and width (Mikhailov et al, 2011). Larger leakoff values result in smaller fractures. Reservoirs that show high leakoff are thus not typically good candidates for an effective and efficient hydraulic fracture treatment. Hydraulic fracturing is therefore usually applied in unconventional or tight oil/gas reservoir with permeability smaller than 1 mD.

Productive geothermal fields like Wayang Windu usually exhibit high leakoff values, compromising the mere success of a hydraulic stimulation. When the induced pressure is sufficient to open the pre-existing fractures, the leakoff will increase by orders of magnitudes because considerable amounts of fluid will instantly flow into the fracture system (Economides & Nolte, 2010). However, numerical and field studies have shown that hydraulic fracture treatments might still be effective if leakoff rate control can be achieved to guarantee sufficient fracture growth. Practical solutions in volcanic environments can be to isolate short

perforated intervals (5-10 meters); to maximize the pump rate; to increase fluid viscosity during the treatment; to use small proppant grain size or to deploy tip-screen-out fracturing (Roodhart et al, 1994; Weijers et al, 2002; Legarth et al, 2005;Weng et al, 2011). Legarth et al (2005) used expansion joints, open hole packers and temporary salt plugs to isolate two intervals of 40 and 60 meters within the open hole completion interval of 420 meters TVD. With a non-aggressive treatment they generated hydraulic fractures that yielded a considerable improvement in production.

The cement design of geothermal wells might currently represent the biggest challenge of the geothermal industry (Salim & Amani, 2013). High-temperature volcanic environments are very challenging and the large wellbore diameters required to accommodate the drilling and pumping tools increase the costs and the technical difficulties (Glauser et al, 2013). Figure 7 sketches how the perforated liner of the Wayang Windu wells is not in contact with the wellbore walls.

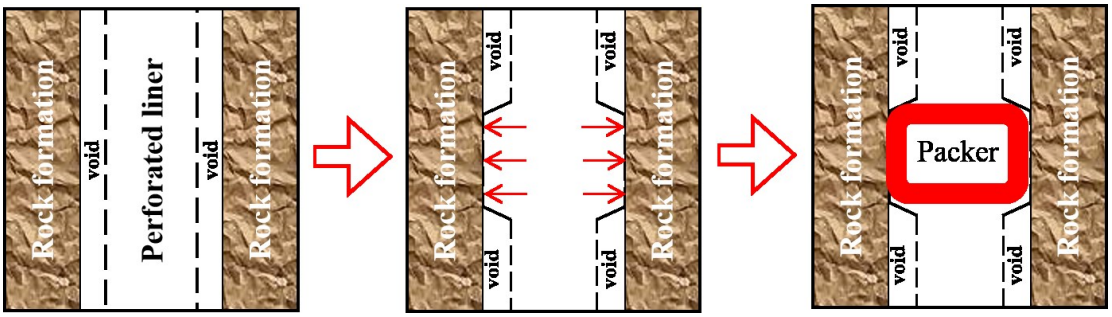

Figure 7. Expanding the perforated liner at the top and base of a short perforated interval will allow to insert an isolating tool, such a packer, and to perform a more effective and safe hydraulic fracture treatment.

The annular empty space makes it difficult to isolate a short section and seriously complicates the design of an effective hydraulic fracture stimulation. To insert inflatable packers or using ball sealers in the perforated liner will not be effective, because the fracture fluid will flow upwards through the annulus. For the same reason, a temporary gel or salt plug might not work. There may be effective solutions, such as expanding the perforated liner to create contact between it and the wellbore walls, or melting and inserting a thermoplast to fill a short section of the annulus. Expanding the liner can be done via hydraulic or inflatable expanders or explosives (Figure 7).

The feasibility of such approaches must be properly tested in a laboratory on casing samples before being applied. The most rigorous, but also most expensive, approach might be to cut the liner and entirely recomplete the well. Then all options available in standard oil and gas applications, including zonal isolation and multi-stage fracturing, become available.

We focus on the stimulation of geothermal wells completed with a long open section with a perforated liner that can only be isolated at the top of the perforated liner. The objective of the stimulation is to connect to the larger fault zones with the 70 m spacing. Therefore, we target fractures of 35 m penetration. As a result, large volumes of fracture fluids and proppant are required, affecting the economic feasibility of the stimulation. Further, the high leak off typical for a densely fractured reservoir will cause a high percentage of the injected fluids to penetrate the formation, reducing the effectiveness of the treatment. Further, because of the effective stress gradient between the top and the base of the perforation interval, the induced fracture is expected to develop only around the top of the perforated liner: the fracture location can thus not be optimized. And finally, there is a potential wellbore integrity issue because of the absence of a cemented annulus. Hydraulic stimulation is associated with the development of large induced stresses. Figure 8 demonstrates how these stresses may activate pre-existing fractures crossing the well and harm the perforated liner via local plastic buckling (Dusseault et al, 2001).

3. METHOD

We have investigated the feasibility of executing an efficient and safe hydraulic fracture treatment on the wells of the Wayang Windu geothermal field with an analytical approach, a single-well reservoir model and a study on wellbore walls failure risk.

3.1 Analysis of injected volumes and fracture efficiency

In this section we provide the mathematical background necessary to evaluate the fluid volumes required to stimulate a hydraulic fracture on the perforated interval of the case study well. The reservoir rock was assumed to have a linear elastic behavior and to be homogeneous. Actual values used in the calculations are listed in Table 6. The required one-wing fracture length of 35 m is based on the 70-m spacing of the large-scale fracture system.

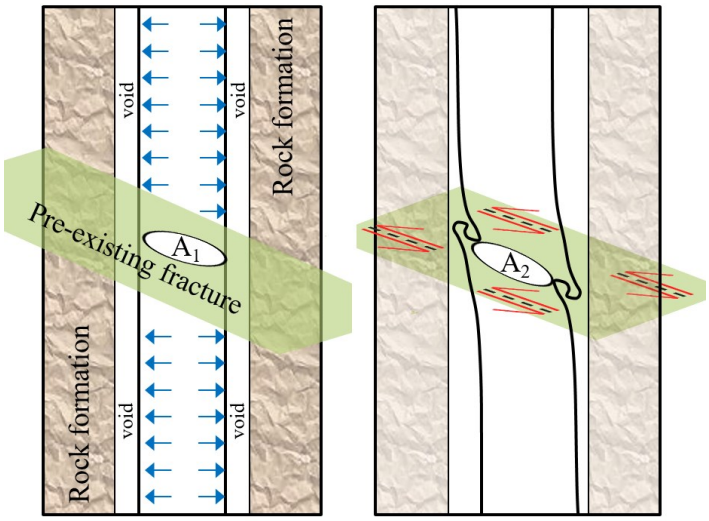

Figure 8. Left: perforated liner crossed by a pre-existing fracture. Right: plastic buckling of the perforated liner induced by the shear displacement of the pre-existing fracture (modified after Dusseault et al, 2001). A_1 and A_2 are the areas of the undeformed and the deformed cross section of the perforated liner respectively.

Table 6. Input data for the analytical calculation. * = related to wellbore section 4 (Table 4). ** = length of section 4 (Table 4).

Well diameter * (j) [m]	0.31 (12" ¼)
Well depth TVD (d) [m]	1279.7
Perforations interval ** (Lint) [m]	710
Fracture height (Hfrac) [m]	710
Fracture length (Lfrac) [m]	35 (per wing)
Injection rate qi [m3/min]	7
Viscosity of the injected fluid m [cp]	0.89

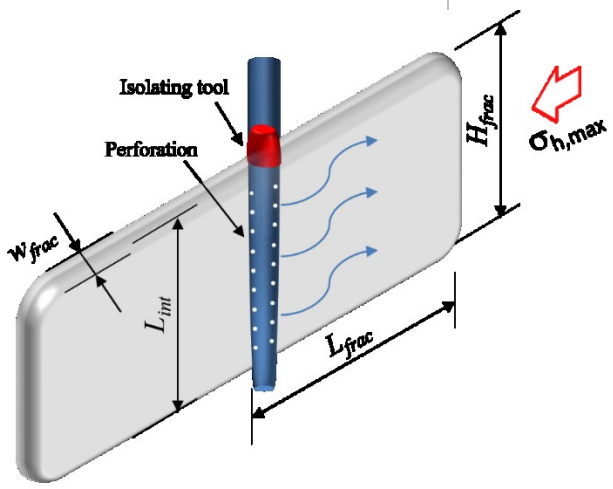

Figure 9. Planar geometry of a 2 wing hydraulic fracture. In this simplified case: $H_{frac} = L_{int}$.

The total volume (V_{frac}) of a 2-wing fracture is calculated assuming a KGD fracture planar shape (Yew & Weng, 2015). This model assumes that the formation is a homogeneous, isotropic and linear elastic medium and that the fracture is simply a channel of opening w_{frac} in a plane-strain state (Figure 9). Such a geometry is an appropriate choice when the fracture length is smaller than the fracture height (Meyer & Bazan, 2011). The fracture volume is given by:

$$V_{frac} = \frac{\pi}{2} \cdot H_{frac} \cdot L_{frac} \cdot w_{frac} \quad (1)$$

It was assumed that an isolating tool could be placed at the top of the perforated liner. The volume (V_{well}) of fluid required to fill the perforated section of the wellbore is not negligible:

$$V_{well} = \pi \cdot \frac{\varphi^2}{4} \cdot L_{int} \quad (2)$$

The total injected volume is:

$$V_{inj} = V_{frac} + V_{well} + V_{leakoff} \quad (3)$$

where $V_{leakoff}$ represents the leakoff volume: the amount of injected fluid lost to the formation without contributing to the fracture volume. An important parameter that gives a qualitative idea of the effectiveness of the hydraulic fracture stimulation is the fracture efficiency. This is defined as (Harrington & Hannah, 1975):

$$\eta = \frac{V_{frac}}{V_{inj} - V_{well}} = \frac{V_{frac}}{V_{frac} + V_{leakoff}} \quad (4)$$

For a specific target value of the fracture volume, the fracture efficiency decreases with increasing leakoff – and vice versa. Generally the fracture efficiency varies during the stimulation because fracture volume and leakoff volume vary differently. The efficiency is highest at the beginning of the treatment. When the hydraulic fracture propagates further into the formation it gradually reduces because of the increasing surface available for the leakoff (Economides & Nolte, 2010).

With a KGD geometry, the dimensions of the hydraulic fracture are calculated following the theory of Perkins and Kern and the total leakoff coefficient, $C_{leakoff}$ with the simplified Carter equation. The fracture length is computed with:

$$L_{frac} = \frac{q_i \cdot w_{frac}}{64 \cdot C_{leakoff}^2 \cdot H_{frac}} \left(e^{S^2} \cdot erfc(S_0) + \frac{2}{\sqrt{\pi}} \cdot S_0 - 1 \right) \quad (5)$$

q_i is the injection rate and the coefficient S_0 can be calculated as a function of the fracture efficiency or of the leakoff coefficient:

$$S_0 = 1.25 \cdot \frac{1-\eta}{\eta} = \frac{8 \cdot C_{leakoff} \sqrt{\pi \cdot t}}{\pi \cdot w_{frac}} \quad (6)$$

where t is the elapsed time after the injection of fluid started expressed in minutes. The width at the well of the fracture is given by:

$$w_{frac} = \left[\frac{84}{\pi} \cdot \frac{\mu \cdot q_i \cdot L_{frac}^2}{E' \cdot H_{frac}} \right]^{\frac{1}{4}} \quad (7)$$

where μ is the viscosity (bar·min) of the injected fluid and E' is the plain strain modulus: $E' = \frac{E}{1-\nu^2}$. Width and length are mutually related by the elastic behavior of the reservoir and the pressure distribution in the fracture. The latter originates from the frictional pressure drop between the entrance at the wellbore and the fracture tip, due to the fluid's high velocity and its viscosity.

3.2 Single-well reservoir model

The aim of the single-well reservoir model was to investigate which treatment design is necessary to develop a hydraulic fracture treatment in the geothermal field and to gain more insight on how a hydraulic fracture will develop in a geothermal environment. To that end, numerical simulations were executed with the numerical simulators MSHALE and MFRAC.

A 3-dimensional fracture model was chosen to obtain a realistic fracture profile (Meyer, 2016). The fractured system of the 70x70 meters structures typical of the Wayang Windu field were modelled in two different ways. The first model explicitly presents the fractured network with D_{frac} = 1.1 m^{-1} and separately considers the low permeability of the rock matrix (0.001 mD). Fluid leakoff is then controlled by the network. The injection well was located in the center of the cluster (Figure 10).

In the second model, the fractures that lie inside the clusters are implicitly considered in terms of enhanced permeability of the rock formation: a higher fracture density will lead to a higher permeability of the rock matrix that is surrounded by the explicitly modelled fractures.

Assuming a laminar flow and no roughness of the fracture walls, the permeability of the implicit fracture network ($k_{impl,DFN}$) is calculated following the cubic law (Whitherspoon et al, 1980).

$$k_{impl,DFN} = \frac{w^3}{12 \cdot S} \quad (8)$$

where w is the width of the pre-existing fractures within the squared clusters of side length L_{clust} and $S = \frac{1}{D_{frac}}$ is the fracture spacing (the distance between 2 adjacent fractures that develop in the same direction). The width of the fracture has three different components (Rutqvist et al, 2004):

$$w = w_{in} + (w_n + w_s) \quad (9)$$

where w_{in} is the initial fracture aperture, w_n is the extra width related to the stress component perpendicular to the fracture surface and w_s is connected to the shear stress. w_n and w_s are induced by stimulation activities: before stimulation: $w_n = w_s = 0$. It was not

possible to acquire field data of the fracture aperture. Therefore a series of sensitivities analysis were run to evaluate the relevance of the initial fracture's aperture.

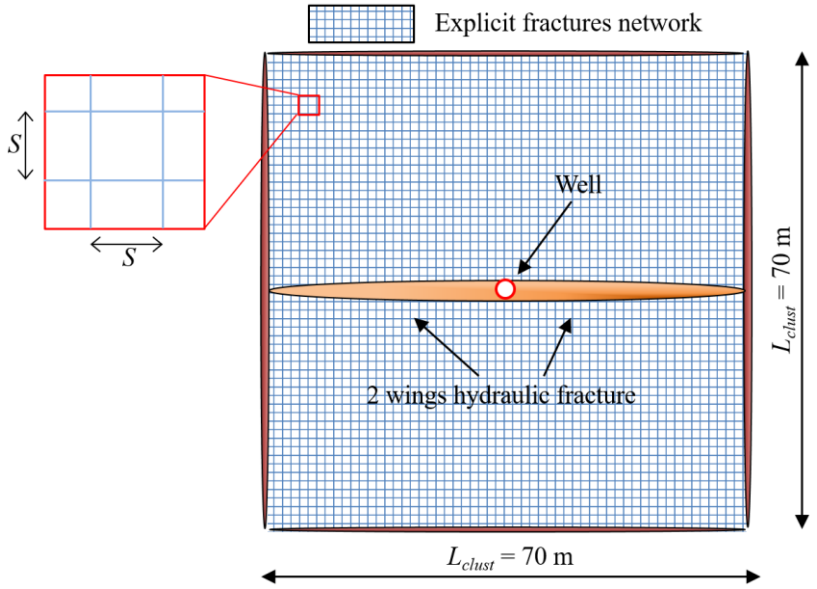

Figure 10. Explicit fractured network within a 70x70 meters cluster.

Table 7. Value of the initial fracture aperture selected for the sensitivities analysis as suggested by Fang et al (2015).

$w_{in,1}$	$5.0e^{-5}$	[m]
$w_{in,2}$	$7.5e^{-5}$	[m]
$w_{in,3}$	$1.0e^{-4}$	[m]

In both cases, two different treatment designs were evaluated. The first focused on the injected volume necessary to develop a 2-wing 70 meters long hydraulic fracture, to evaluate if the total volumes of fracture fluid and proppant and the power required were technically and economically feasible. The interest of the second was to assess the hydraulic fracture that could be stimulated with a treatment design of 500 m^3 of injected fluid (400 m^3 of pad stage, 100 m^3 of proppant stage, 9.6 kg/ m^3 of proppant concentration).

The total leakoff coefficients of the rock matrix and of the fractures are controlled by different mechanisms. The leakoff of the rock matrix is a function of the reservoir properties, such as permeability, porosity and compressibility. The fracture leakoff depends on the pressure gradient between the formation pressure and the pressure within the fracture and it is not connected to the matrix properties (Barree et al, 2009).

Table 8. Perforation zone data.

Zone	Top perfs MD	Bottom perfs MD	Perforations number	Perforations diameter
	[m]	[m]		[mm]
Perforated liner	890	1600	922	9.9

Following the work of Weijers et al (2002) and Weng et al (2011), a smaller proppant grain size was selected to optimize the placement and increase the durability of the proppant (30/50 SinterBall Bauxite).

In all the numerical simulations performed with the single-well reservoir model we assumed that it was possible to introduce an isolating tool on top of the perforated liner.

3.3 Analysis of the wellbore failure risk

Trying to induce a hydraulic fracture might also compromise the wellbore integrity. Expressions to calculate the well pressures required to reach shear or tensile failure of the borehole walls have been presented by Fjaer et al (2008). These equations were formulated for idealized conditions, but they are useful to draw a clearer picture of the risk of damaging the wellbore. Breakouts along the shear bands (Figure 11, right) will occur if the pressure inside the well is below the shear limit ($p_{well,min}$):

$$p_{well,min} = p_{form} + \frac{\sigma_V + 2\upsilon\,(\sigma_{h,max} - \sigma_{h,min}) - p_{form} - C_0}{(\tan\beta)^2} \quad (10)$$

where C_0 and β are the uniaxial compressive strength and the failure angle of the rock formation, respectively. The breakouts will propagate in the direction of $\sigma_{h,min}$.

Tensile fracturing will occur when the pressure inside the wellbore is greater than the tensile failure limit:

$$p_{well,max} = 3\sigma_{h,min} - \sigma_{h,max} - p_{form} + T_0 \quad (11)$$

where T_0 is the tensile strength of the rock formation. The actual tensile strength of the rock formation in the near well area is negligible ($T_0 = 0$) because of the damaged zone created by the drilling process. Equation (12) should be used to evaluate fracture initiation and propagation only in the stress concentration area: approximately within one well diameter of distance from wellbore wall. Outside this near-wellbore zone, we used the propagation criterion for tensile fractures given by:

$$p_{well,max} = \sigma_{h,min} + T_0 \quad (12)$$

where the tensile strength $T_0 \neq 0$ because here the rock formation is assumed intact.

The values calculated with equations (10) and (11) give the range of wellbore pressures needed to ensure the integrity of the wellbore. The in situ horizontal stresses of the Wayang Windu field present a strong anisotropy: $\sigma_{h,max} \cong 2\,\sigma_{h,min}$. Such a large anisotropic stress field decreases the range of pressures for which the wellbore walls are stable (higher $p_{well,min}$ and lower $p_{well,max}$). Moreover, because $\sigma_{h,max} \gg \sigma_{h,min}$, the pressure calculated with equation (12) might be lower than tensile failure criterion outside the stress concentration area.

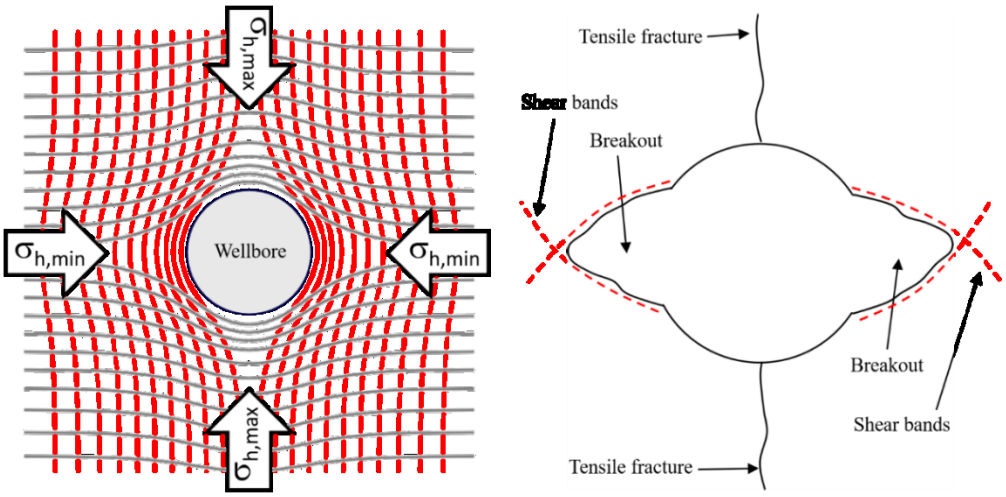

Figure 11. Left: top view of the stress field around a wellbore. The grey and red lines show the stress field (combination of the horizontal in situ stress). The presence of the wellbore creates stress concentration areas in the direction of the horizontal stresses. Right: Top view of the damages that can occur on the wellbore walls. In the Wayang Windu field a marked anisotropy in the horizontal stress is measured. This leads to wellbore breakouts that develop along shear bands in the direction of the minimum horizontal stress. During drilling, too high mud pressures can induce tensile fractures in the direction of the maximum in situ stress.

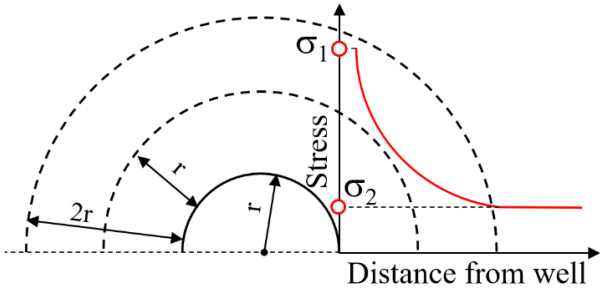

Figure 12. Simplified sketch of the stress field area around the wellbore. σ_1, σ_2 = horizontal stress, σ_3 = vertical stress. At the distance of approximately one well diameter from the wellbore wall, the stress returns to its unperturbed state (far field stress, σ_2). Closer to the wellbore, the stress is much higher than the far field stress: $\sigma_1 \cong 3\,\sigma_2$.

A large anisotropy of the horizontal in situ stresses will entail higher pressure to open pre-existing fractures. The wellbore net pressure is defined as the pressure required to open a pre-existing fracture in the direction of the maximum horizontal stress and it is given by Nolte & Smith (1981):

$$p_{openDFN} = \frac{\sigma_{h,max} - \sigma_{h,min}}{1 - 2v} \quad (13)$$

High values of $p_{openDFN}$ have both a positive and negative effect on the hydraulic fracture stimulation. If the width of the pre-existing fractures is not increased by the overpressure, the leakoff of the fractured geothermal system stays to a more acceptable level and the induced hydraulic fracture can penetrate deeper into the reservoir. On the other hand, if the pre-existing fractures do not open, the effectiveness of the stimulation will be more limited.

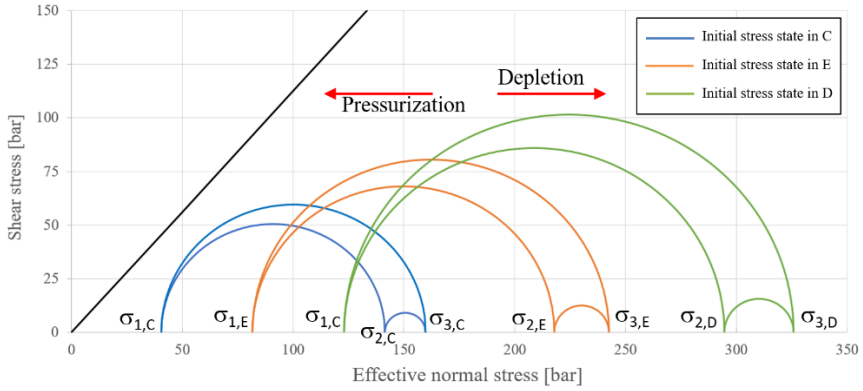

Figure 13. Visualization via Mohr-Coulomb circles of the initial state of stress of 3 different points of the geothermal reservoir (Figure 2). C: top of the reservoir, D: base of the perforated liner, E: center of the perforated liner. In absence of field data, it has been adopted a friction angle of 60° and zero cohesion is assumed. σ_1 = minimum horizontal stress, σ_2 = vertical stress, σ_3 = maximum horizontal stress.

The analysis of the shear failure of the perforated liner (Figure 8) is performed via Mohr-Coulomb theory. The initial state of stress of 3 different locations of the reservoir was considered: at the top, in the middle and at the end of the perforated liner (Figure 2). Inducing an overpressure in the reservoir will destabilize the pre-existing fractures around the injection well by moving the Mohr circle closer to the failure line (Figure 13).

4. RESULTS

4.1 Analysis of injected volumes and fracture efficiency

Equations (1-8) allow a first estimate of the amount of fluid volumes needed to stimulate a 2-wings hydraulic fracture. For a hydraulic fracture of 35 m long per wing and height equal to the perforated length (710 m) we obtained an average width of 1.0 mm (Eq. 7 and 8; Table 8). The width is limited because of the extended length of the perforated interval. Figure 14 (left) shows the results for the total volume of injected fluid that is needed to develop a tensile fracture along the complete perforated interval: L_{int} = H_{frac} = 710 m. Figure 14 (right) shows the dependence of the required volumes on fracture height – also indicating the range of lengths of perforated intervals found in Wayang Windu.

For low fracture efficiency, the volume needed is very high. While the gap between η = 100% and η = 50% is limited, the disparity between the volume needed when η = 50% and when η = 10% is pronounced. Because of the dense fracture network that characterizes the Wayang Windu geothermal field, the leakoff coefficient of the rock formations is expected to be high. Based on experience and data collected from literature, the fracture efficiency (η) will be between 7% and 15%. For such values the required fluid volume is expected to strongly affect the economic profitability of the stimulation.

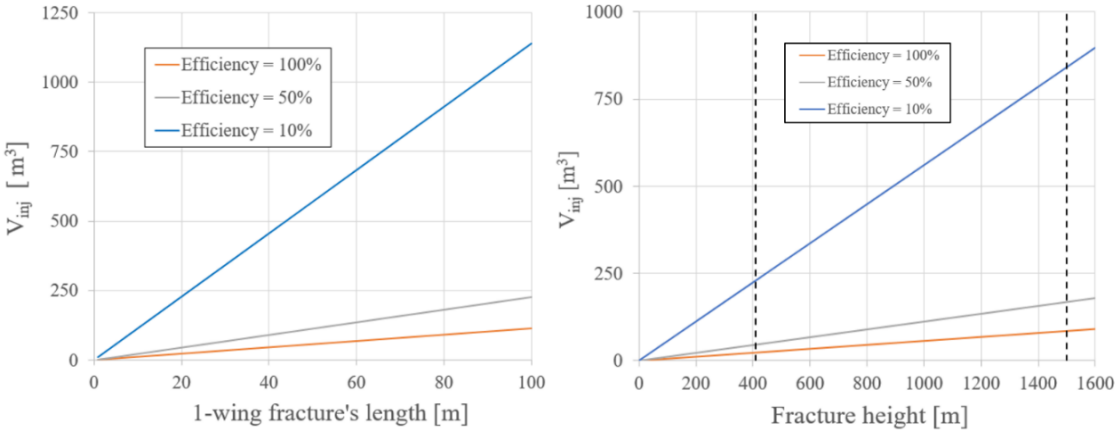

Figure 14. Left: total volume of injected fluid (V_{inj}) necessary to stimulate a hydraulic fracture 710 meters high and 1.0 millimeters wide as a function of the fracture half-length and for different fracture efficiencies. Right: total volume of injected fluid (V_{inj}) necessary to stimulate a hydraulic fracture 35 meters long and 1.0 millimeters wide as a function of the perforated interval length (assuming L_{int} = H_{frac}) and for different fracture efficiencies. The dashed black lines represent the shortest and longest perforated intervals that can be found in the wells of the Wayang Windu field.

The fracture efficiency strongly affects the demanded amount of fracturing fluids. Fixing the geometries of the well and the hydraulic fracture (⇒ V_{well} and V_{frac} are constant), the total injected fluid volume depends only on the leakoff volume (equation (3)). The injected volume grows very fast for low values of the fracture efficiency (Figure 15).

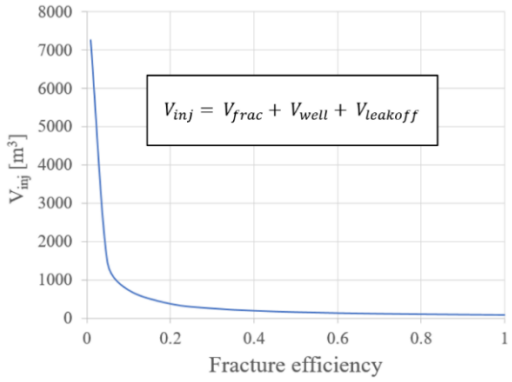

Figure 15. Fluid volume needed to stimulate hydraulic fractures of the geometry showed in Table 6 as a function of the fracture efficiency.

4.2 Single-well reservoir model

We described in Section 3.2 the two different single-well reservoir models: the first with an explicitly modelled dense fracture network and the second with an implicitly modelled fracture network in terms of homogenized rock matrix permeability.

For the explicitly modelled fracture network, two scenarios with diverse treatment designs were analyzed. In the first, the input was given by the target length of one wing of the hydraulic fracture and the injection rate (q_i = 7 m^3/min). In the ideal situation in which the injection well was placed in the middle of a fractured cluster, we chose L_{frac} = 35 meters (Figure 16) – again based on the 70-m spacing of the large-scale fracture system. The required injected volume to stimulate a 35 meters long fracture in the dense fracture network is 260 m^3 and the BHTP is 180 bars.

For the second scenario we investigated the sensitivity of the treatment to the stimulation design by calculating the dimensions based on a range of injection volumes and injection rates. First, input was only given by the injection rate (q_i = 7 m^3/min) and a wide range of injection volumes were considered (Figures 17 and 18). In both scenarios a proppant distribution allocation was selected: the ratio between the proppant mass staying in the induced hydraulic fracture and the total mass was taken 50%. The background of this choice is the extended leakoff, causing the proppant not to stay in high percentages in the main fracture but also spreading into the fracture network near the induced hydraulic fracture.

The sensitivity to the injection rate was also investigated (Table 9). In the range of injection rates evaluated, the length of the calculated hydraulic fractures is similar (32 – 35 m). The leakoff rate is high in all the cases: ~98 % of the injection rate towards the end of the treatment. The induced hydraulic fracture is not confined in the interval of the perforated liner but it propagates above the top of the reservoir. The fracture efficiency keeps decreasing during treatment for all scenarios.

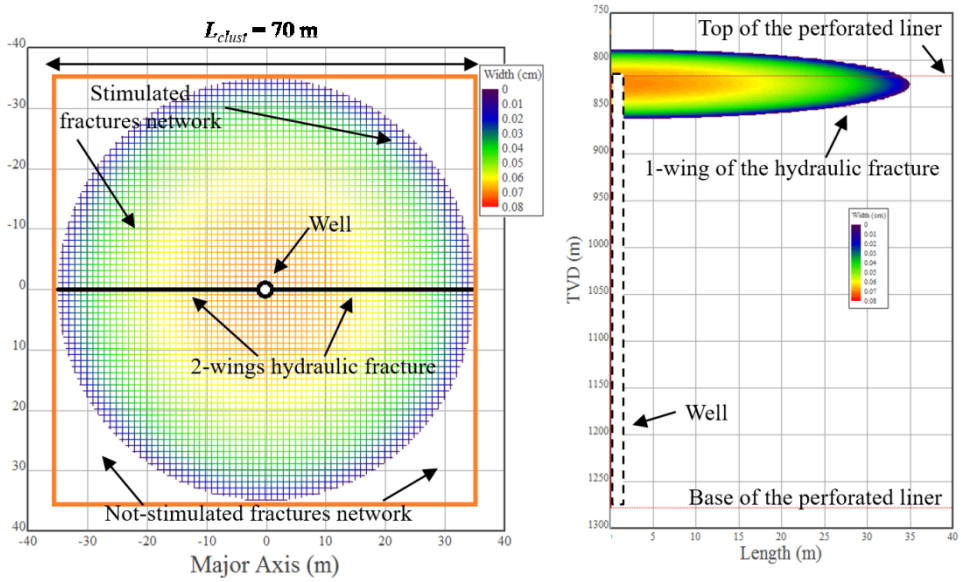

Figure 16. Left: top view of the 2-wings hydraulic fracture and of the stimulated fracture network within a 70x70 meters cluster. The color plot shows the width of the fractures after stimulation. Right: side view of one of the wing of the hydraulic fracture. In this case: L_{frac} = 35 m (input), H_{frac} = 74.7 m. The color plot shows the width of the stimulated hydraulic fracture at the end of hydraulic fracture treatment.

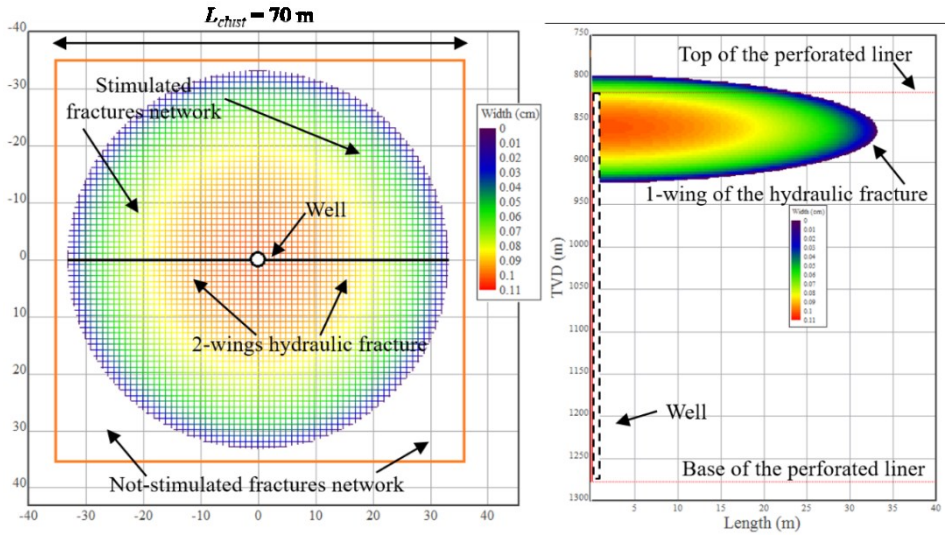

Figure 17. Left: top view of the 2-wings hydraulic fracture and of the stimulated fracture network within a 70x70 meters cluster (V_{inj} = 500 m^3, q_i = 7 m^3/min). The color plot shows the width of the fractures after stimulation. Right: side view of one of the wings of the hydraulic fracture. The color plot shows the width of the stimulated hydraulic fracture at the end of hydraulic fracture treatment.

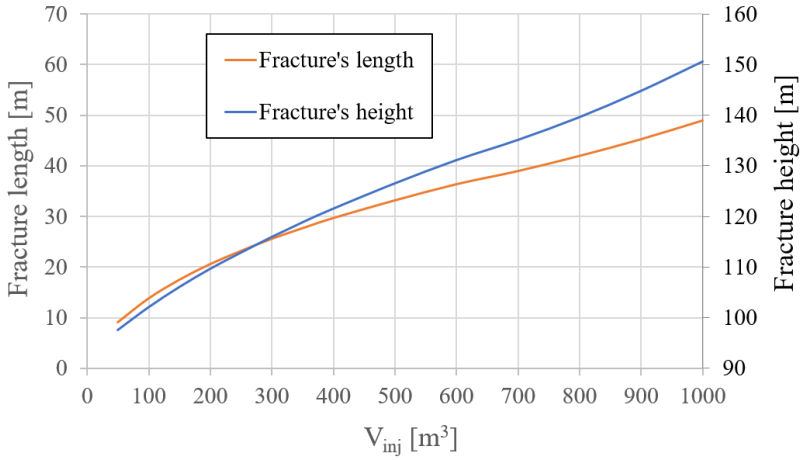

Figure 18. Explicit fracture network scenario. Length and height of the induced hydraulic fracture for different injection volumes at fixed injection rate (q_i = 7 m^3/min).

Table 9. Characteristic of the stimulated hydraulic fracture for the different injection rate and constant injected volume (500 m^3). * = 1 wing length. ** = initial and end of final (EOJ) efficiency of the main fracture. LOR = leakoff rate. BHTP = bottom hole treating pressure. In all analyzed cases the fracture propagates 20-30 meters above the top of the perforated liner and stay confined in the transition zone.

q_i [m^3/min]	L_{frac}[m]*	H_{frac} [m]	LOR [m^3/min]	η [%] **	BHTP [bar]
1	35.3	121.5	0.99	16 – 1.2	165.8
3	33.8	127.5	2.99	30 – 1.5	168.9
5	33.5	126.8	4.92	23.5 – 1.6	170.8
7	33.2	126.5	6.94	19.5 – 1.7	172
9	32.9	126	8.89	19 – 1.7	173.4
11	32.6	125.5	10.8	19 – 1.8	174.1

For the implicit fracture network we followed equations (9) and (10) to calculate the permeability of the implicit fracture network ($k_{impl,DFN}$) as a function of the fracture density (Figure 19). A fracture density of 1.1 m^{-1} was selected to evaluate the fracture

dimensions for a fixed injected volume and rate (V_{inj} = 260 m^3, q_i = 7 m^3/min). In this case the proppant was assumed to stay in the induced tensile fracture because the fracture network was not physically modeled.

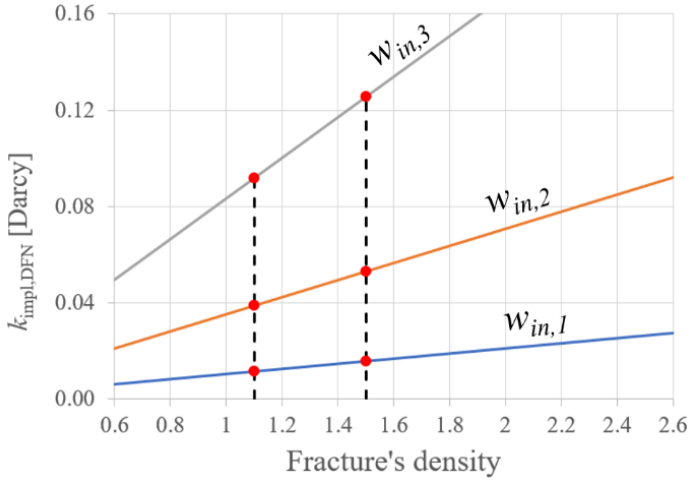

Figure 19. Permeability of the implicit fracture network ($k_{impl,DFN}$) as a function of the fracture density for different initial fractures' aperture.

Table 10. Calculated permeability of the implicit fracture network for different initial aperture of the pre-existing fractures. * = average fracture density of the Wayang Windu field.

Initial fracture width	$k_{impl,DFN}$ [Darcy]	
	D_{frac} = 1.1 m^{-1}	*D_{frac} = 1.5 m^{-1}
$w_{in,1}$	0.012	0.016
$w_{in,2}$	0.038	0.053
$w_{in,3}$	0.092	0.125

Table 11. Characteristic of the stimulated hydraulic fracture for the different permeability of the implicit fracture network with constant injected volume (260 m^3). * = 1 wing length. LOR = leakoff rate. BHTP = bottom hole treating pressure.

w_{in}	L_{frac}*	H_{frac}	LOR	BHTP
[m]	[m]	[m]	[m^3/min]	[bar]
5.0e^{-5}	49	165.7	5	150
7.5e^{-5}	48.8	165.1	5.03	150
1.0e^{-4}	48.6	164.8	5.05	150

The high permeability of the homogenized rock matrix did not seem to limit the development of the stimulated fracture in comparison to the case of the explicitly fractured network. However, the hydraulic fracture strongly developed above the top of the perforated liner (Figure 20). The calculated geometry and characteristics of the induced hydraulic fracture did not significantly change upon the use of the three different initial fracture apertures (Table 11).

4.3 Analysis of the wellbore failure risk

The magnitudes of the well pressures needed to develop shear breakouts or to propagate tensile fractures within the steam zone of the geothermal reservoir were calculated by solving equations (11), (12) and (13). The results are presented in Figure 21.

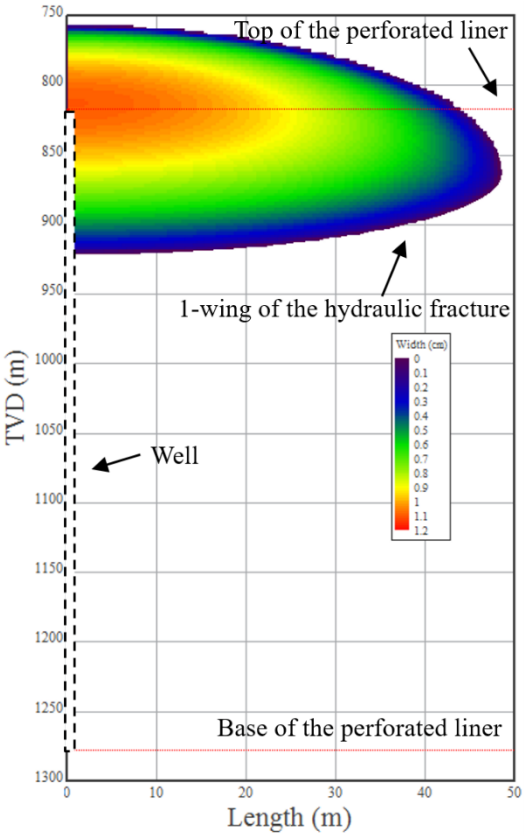

Figure 20. Side view of one of the wing of the hydraulic fracture. In this case the fractured network was modelled implicitly: L_{frac} = 48.6 m (input), H_{frac} = 164.8 m. The color plot shows the width of the stimulated hydraulic fracture at the end of hydraulic fracture treatment.

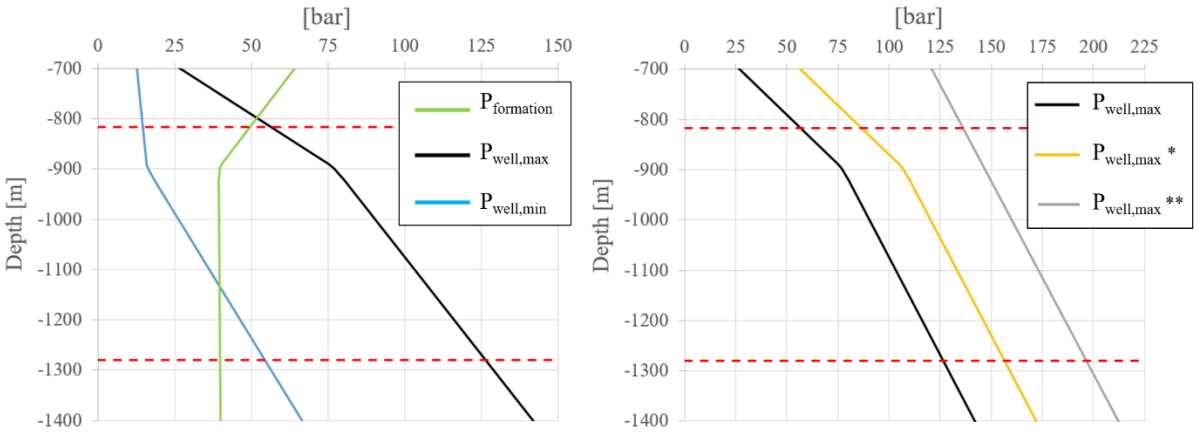

Figure 21. The dashed red lines indicate the top and the base of the uncemented perforated liner. Left: well pressures needed to generate breakout (blue line) and propagate tensile fractures (black line) with the damaged zone around the wellbore wall. Right: well pressure needed to originate tensile fracture within the near wellbore damaged zone (black line), within the damaged zone if the tensile strength in not zero, T_0 = 30 bar (*, yellow line), and outside the damaged area (, grey line).**

The pressure within the dry steam geothermal reservoir is almost constant (Figure 21, left, green line) because of the low hydrostatic pressure gradient of the steam (0.0017 bar/m). At depths greater than approximately 1130 meters, the formation pore pressure is smaller than the minimum wellbore pressure needed to not damage the wellbore walls. Such behavior originates from the strong anisotropy of the in-situ horizontal stress, which creates intense stress concentration in the near wellbore area. Above the top of the reservoir, the formation pore pressure is larger than the maximum allowed pressure under the assumption of zero tensile strength, but since the well is cased there this does not pose a risk. Outside the stress concentration zone (approximately one wellbore diameter of distance from the wellbore wall), the pressure needed to propagate tensile fractures is much higher (Figure 21, right, grey line). Far from the wellbore the magnitude of the maximum horizontal stress is not relevant in the analysis of the stability of the wellbore walls. Moreover, because the rock formation is considered not damaged by the drilling process, the tensile strength of the rock is not negligible ($T_0 \neq 0$).

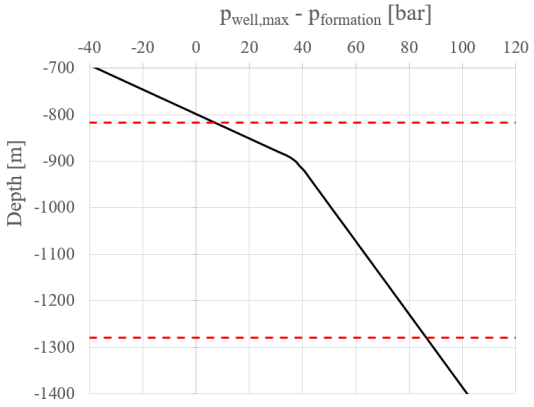

Figure 22. Difference between the formation pore pressure and the well pressure needed to propagate tensile fractures ($p_{well,max}$). The dashed red lines indicate the top and the base of the uncemented perforated liner.

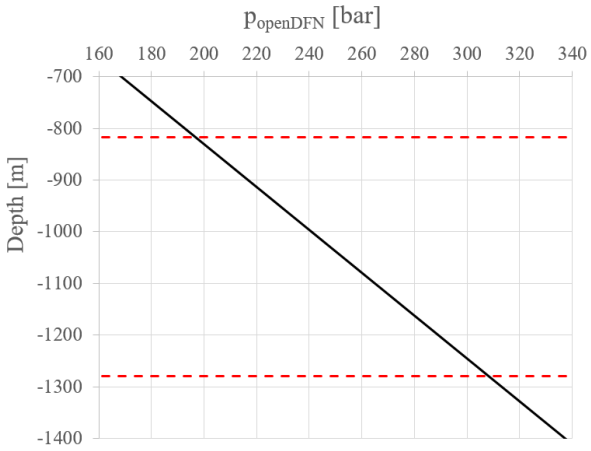

Figure 23. Well pressure required to enhance the width of the existing fractures. The dashed red lines indicate the top and the base of the uncemented perforated liner.

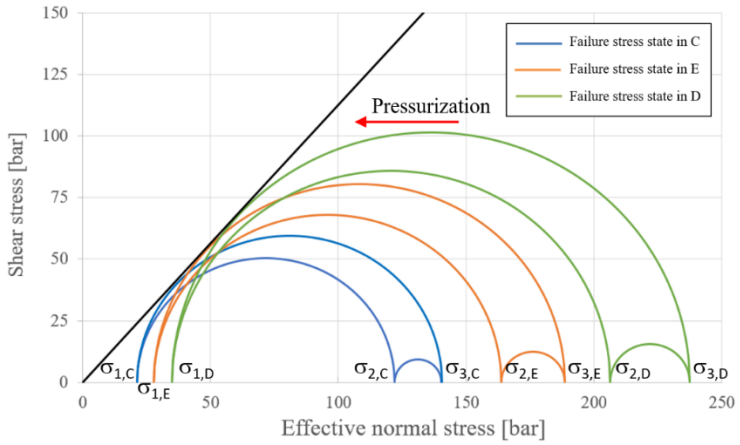

Figure 24. Visualization via Mohr-Coulomb circles of the state of stress at failure of 3 different points of the geothermal reservoir (Figure 2). C: top of the reservoir, D: base of the perforated liner, E: center of the perforated liner. In absence of field data, it has been adopted a friction angle of 60°. σ_1 = minimum horizontal stress, σ_2 = vertical stress, σ_3 = maximum horizontal stress.

The pressures evaluated can now be used to identify pressure conditions risking tensile failure. The condition is in the range of 5 and 40 bars in the section of the perforated liner close to the reservoir top (Figure 22). Further, from equation (14) we quantified the well pressure necessary to open the pre-existing fractures of the geothermal field. Because of the high anisotropy of the horizontal in situ stresses ($\sigma_{h,max} >> \sigma_{h,min}$), these are relatively high: 200-300 bar (Figure 23).

We finally employed Mohr-Coulomb theory to calculate the overpressure necessary to reactivate pre-existing fractures in the rock matrix around the injection well. For the failure envelope we used a friction angle of 60° and zero cohesion. Table 12 provides the numbers to move the initial stresses (Figure 13) to critical state (Figure 24).

Table 12. Magnitudes of the overpressures (pressure of the injected fluid above the formation's pressure) needed to shear pre-existing fractures (Δp_{shear}) and to open new tensile fractures (Δp_{frac}) at 3 different depths in the geothermal reservoir. References of the location of points C, D and E can be found in Figure 2.

Point	Depth	pformation	Dpshear	Dpfrac
	[mTVD]	[bar]	[bar]	[bar]
C	917	78.6	19.4	31.4
E	1237	79.1	53.8	70.9
D	1560	79.7	88.3	112.8

In all cases $\Delta p_{frac} > \Delta p_{shear}$: shear displacements will occur before opening new tensile fractures, increasing the chances of damaging the wellbore stability.

5. DISCUSSION

5.1 Efficiency of hydraulic stimulation

The Wayang Windu field is characterized by a high fracture density. For this reason a low fracture efficiency is expected. Still, fracture lengths of the order of 35 m must be created to connect to the large-scale fracture structures that constitute the main flow system. As shown in Figure 14, the injected fluid volume that it is required to stimulate a tensile fracture of that length increases rapidly when lowering the values of the fracture efficiency. Also, high injection rates will be required. And, even while commercial hydraulic pumps can reach rates higher than 2000 GPM (7.6 m^3/min), building the necessary overpressure in the well quickly enough to induce a long enough hydraulic fracture before the fracture fluid gets lost in the fractured network, it seems to be a technical issue that is hard to overcome.

Two important issues are not covered in the analytical formulas. The first is that the efficiency is a function of time. This can be addressed by making time-dependent calculations, as was done with the single-well models. The second issue is that the fracture is assumed to cover the full height of the perforated section. This is also addressed by the single-well models.

A single-well reservoir model was employed to the fractured geothermal reservoir around the case study well. Two models were created: with an explicitly and with an implicitly modelled fractured network. A tensile fracture reaching the extremes of the 70x70 meters cluster appeared to be technically feasible for a single-stage fracture treatment, but the dense fracture network around the injection well leads to a very low fracture efficiency. This is in accordance with the analytical calculations. The consequence is that proppant placement will be problematic.

The specific results of the models with the explicit and with the implicit fracture network were very different. This is particularly clear when comparing the fracture efficiencies resulting from the two approaches (Figure 25). The difference is related to the difference in modelling approach: an explicitly modelled fracture network allows the network to open progressively and is therefore more realistic. Modelling the geothermal reservoir as an homogeneous rock matrix leads to a wrong evaluation of the fracture's efficiency and overestimates the length and height of the induced hydraulic fracture. It is better to deploy the case with the explicitly modelled fracture network.

More importantly, in all the studied scenarios with the single-well model the induced hydraulic fracture propagates above the top of the reservoir up to few tens of meters and it does not penetrate the deeper parts of the reservoir (Figures 16, 17, 19). The bottom hole pressure that is reached while developing a hydraulic fracture on the shallower part of the perforated liner is not sufficient to propagate a hydraulic fracture all the way to the base of the liner. This is a serious problem because a deeper penetration into the geothermal reservoir is required to significantly improve the connection with the pre-existing fractures and the associated productivity of the well.

A hydraulic fracture treatment would be much more effective if it would be possible to isolate a shorter perforated interval, for example by expanding the perforated liner to create a contact with the wellbore wall and introducing sealing packers (Figure 7). Then it would be possible to target the part of the geothermal reservoir that would benefit most from the stimulation procedure. Figure 26 shows the fracture dimensions resulting from the same treatment design on a shorter perforated interval (20 meters) with the same perforation spacing and diameter, halfway the original open section. A hydraulic fracture 42 meters deep and 84 meters high could be induced. Also here, the efficiency of the fracture is extremely low: it varies between 4.5% and 1% at the end of the stimulation. The isolation of a limited interval in the open hole section with the perforated liner, however, is not at all trivial and is not yet standard industry practice. Failure of the perforated liner is a realistic risk. Application of zonal isolation in these types of completions will therefore require extensive prior laboratory tests.

The uncertainties in our input parameters are considerable, therefore so are the uncertainties in the quantitative results of the calculations. This does, however, not compromise the qualitative results: the large leakoff values in combination with the long open sections challenge the mere possibility of effectively fracturing these kinds of reservoirs.

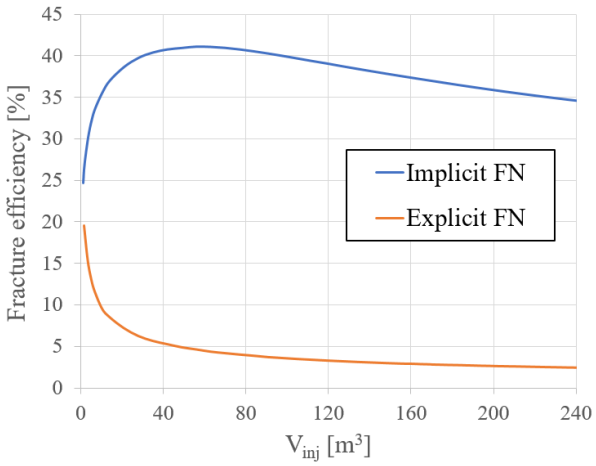

Figure 25. Evolution of the efficiency of the induced hydraulic fracture during injection if the fractured network (FN) is explicitly (orange line) or implicitly model (blue line) when V_{iinj} = 220 m^3, q_i = 7 m^3/min.

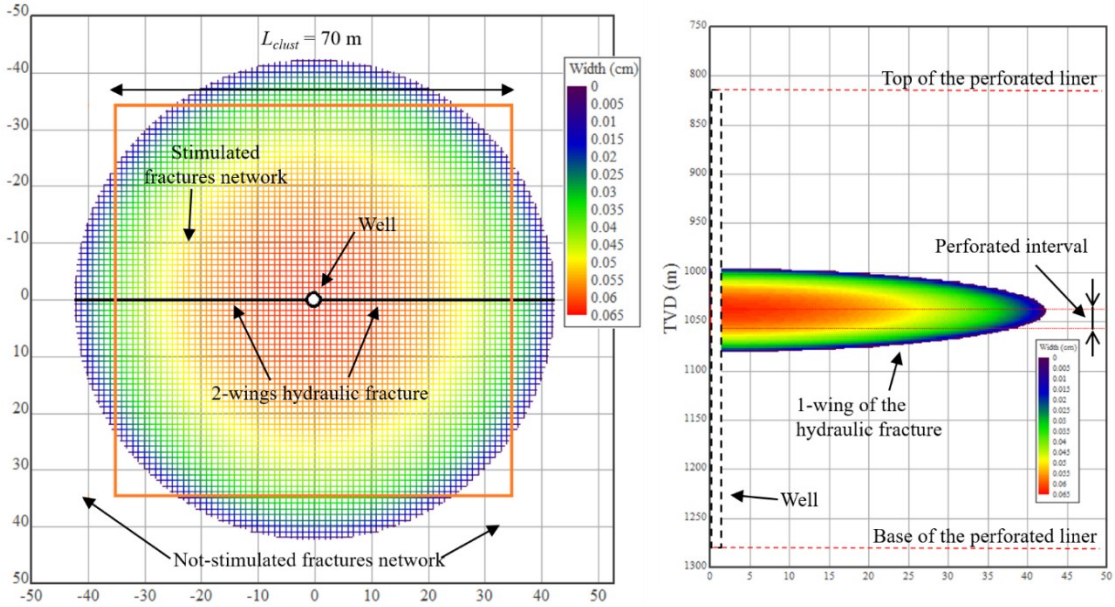

Figure 26. Left: top view of the 2-wings hydraulic fracture and of the stimulated fracture network (V_{inj} = 260 m^3, q_i = 7 m^3/min). The color plot shows the width of the fractures after stimulation. Right: side view of one of the wing of the hydraulic fracture. In this case: L_{frac} = 42 m, H_{frac} = 84 m. The color plot shows the width of the stimulated hydraulic fracture at the end of fracture treatment.

5.2 Analytical study on wellbore wall failure risk

Working on a long perforated interval is also challenging because the in situ stress increases significantly with the depth while the pore pressure is approximately constant (Figure 21, left). As a result, the section is prone to tensile failure at the top and to shear failure at the bottom. Increasing the pressure to propagate a hydraulic fracture can thus cause well failure, especially in the lower part of the open hole section. Moreover, the absence of cement, in combination with high differential stresses and the high fracture densities that are typical in the Wayang Windu field, increase the chances of plastic buckling. Buckling will irremediably reduce the cross section of the perforated liner and compromise its integrity and can ultimately lead to a disconnection of parts of the geothermal reservoir.

The well pressure needed to propagate tensile fractures outside the stress concentration area is much higher than the well pressure needed to propagate such fractures in the stress concentration annulus (Figure 21, right). As a result, an annulus of thickness up to one well diameter might already collapse into the wellbore before the overpressure has been reached the value necessary to propagate a tensile fracture. Moreover, the high horizontal-stress anisotropy makes it difficult to open the pre-existing fractures. Figure 27 shows how the overpressure required to open the fractured network is much higher than the overpressure needed to develop tensile fracture in the stress concentration annulus, even if we consider the near wellbore area to be not damaged (T_0 = 30 bars, blue line).

If it is not possible to isolate a short interval of the perforated liner, the technical issues together with the risk of irremediably damaging the wellbore, should drive the choice of the proper stimulation technique towards other possibilities than hydraulic fracturing.

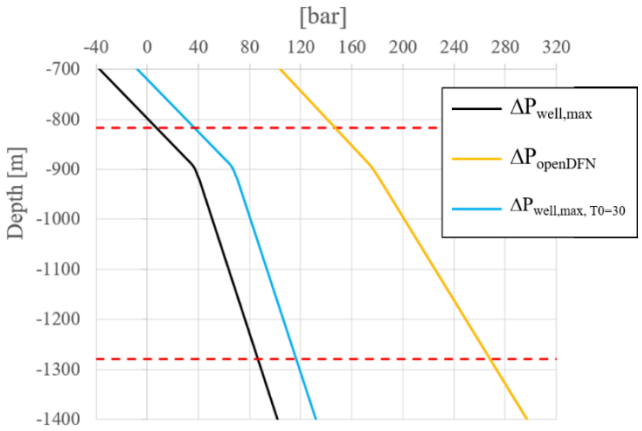

Figure 27. Overpressure ($\Delta P_{well,max} = P_{well,max} - P_{formation}$) needed to develop tensile fractures along the wellbore wall (black and blue, if T_0 = 30 bars, lines) and overpressure ($\Delta P_{openDFN} = P_{openDFN} - P_{formation}$) required to effectively stimulate the fracture network (yellow line). The dashed red lines indicate the top and the base of the uncemented perforated liner.

6. CONCLUSIONS

The focus of this work was to investigate whether hydraulic fracturing could be the proper stimulation technique to improve production of sub-commercial wells of the Wayang Windu geothermal field (West Java, Indonesia), as applying the right stimulation approach can push the production to the desired level. However, performing a fracture treatment in volcanic environments like these presents several challenges. We have investigated technical and geological issues affecting the effectiveness and efficiency of hydraulic fracturing. The impracticality of appropriately isolating a short section of the perforated liner appeared to be the biggest concern. In all studied scenarios, it was possible to propagate a hydraulic fracture, but only in a constrained area at the top of the perforated liner. The simulated fracture were also propagating vertically slightly above the top of the reservoir into the clay cap for a few tens of meters.

We also demonstrated how the execution of a hydraulic fracture treatment on a long perforated interval (400-1500 m) can jeopardize the integrity of the well. This is related to the large differences in stresses along the open well path.

If isolation of a short section of the perforated liner is not technically possible or economically too expensive, hydraulic fracturing might not be the correct stimulation technique. The high leakoff of the dense fracture system in combination with the large stress differences along the perforated section length make the Wayang Windu a bad candidate to perform a hydraulic fracture stimulation.

The high injectivity that causes the high fracture leakoff can also be exploited to apply alternative stimulation approaches. For example, if the pressure and temperature fronts of high volumes of injected fluid can quickly penetrate deeply into the reservoir, thermal and acid stimulations can be a valuable alternative to hydraulic fracture stimulation.

ACKNOWLEDGEMENTS

This work was part of the Geocap project (Geothermal Capacity Building Program Indonesia - Netherlands), an international collaboration between Indonesian and Dutch partners (https://www.geocap.nl/), funded by the Ministry of Foreign Affairs of the Netherlands. In particular, it was the outcome of a collaboration between TNO (NLD) and Star Energy (IND).

REFERENCES

Barree, R. D., Barree, V. L., & Craig, D. (2009). Holistic fracture diagnostics: consistent interpretation of prefrac injection tests using multiple analysis methods. SPE Production & Operations, 24(03), 396-406.

Bogie, I., Kusumah, Y. I., & Wisnandary, M. C. (2008). Overview of the Wayang Windu geothermal field, West Java, Indonesia. Geothermics, 37(3), 347-365.

Cumming, W. (2009, February). Geothermal resource conceptual models using surface exploration data. In Proceedings. SGP-TR-187, Stanford, 2009.

Dusseault, M. B., McLennan, J., & Shu, J. (2011). Massive multi-stage hydraulic fracturing for oil and gas recovery from low mobility reservoirs in China. Petroleum Drilling Techniques, 39(3), 6-16.

Dusseault, M. B., Bruno, M. S., & Barrera, J. (2001). Casing Shear: Causes, Cases, Cures. SPE Drilling & Completion, 16(02), 98-107.

Economides, M.J. & Nolte, K.G. Reservoir Stimulation, Book, Wiley, 2010.

Fang, Y., Elsworth, D., & Cladouhos, T. T. (2015). Estimating in-situ permeability of stimulated EGS reservoirs using MEQ moment magnitude: an analysis of Newberry MEQ data. In Proceedings, 40th Workshop on Geothermal Reservoir Engineering, Stanford University.

Fauzi, A., Permana, H., Indarto, S., & Gaffar, E. Z. (2015, April). Regional structure control on geothermal systems in West Java, Indonesia. In Proceedings World Geothermal Congress, Melbourne, Australia (pp. 19-25).

Fjaer, E., Holt, R. M., Raaen, A. M., Risnes, R., & Horsrud, P. (2008). Petroleum related rock mechanics (Vol. 53). Elsevier.

Glauser, W., McLennan, J., & Walton, I. (2013, May). Do perforated completions have value for engineered geothermal systems. In ISRM International Conference for Effective and Sustainable Hydraulic Fracturing. International Society for Rock Mechanics and Rock Engineering.

Han, H., Dusseault, M., Xu, B., & Peng, B. (2006, January). Simulation of Tectonic Deformation and Large Area Casing Shear Mechanisms----Part B: Geomechanics. In Golden Rocks 2006, The 41st US Symposium on Rock Mechanics (USRMS). American Rock Mechanics Association.

Harrington, L., & Hannah, R. R. (1975, January). Fracturing design using perfect support fluids for selected fracture proppant concentrations in vertical fractures. In Fall Meeting of the Society of Petroleum Engineers of AIME. Society of Petroleum Engineers.

Heap, M. J., Wadsworth, F. B., Xu, T., & Chen, C. F. (2016). The strength of heterogeneous volcanic rocks: a 2D approximation. Journal of Volcanology and Geothermal Research, 319, 1-11.

Hochstein, M. P., & Sudarman, S. (2008). History of geothermal exploration in Indonesia from 1970 to 2000. Geothermics, 37(3), 220-266.

Howard, G. C., & Fast, C. R. (1957, January). Optimum fluid characteristics for fracture extension. In Drilling and Production Practice. American Petroleum Institute.

Legarth, B., Huenges, E., & Zimmermann, G. (2005). Hydraulic fracturing in a sedimentary geothermal reservoir: Results and implications. International Journal of Rock Mechanics and Mining Sciences, 42(7-8), 1028-1041.

Masri, A., Barton, C., Hartley, L., & Ramadhan, Y. (2015, January). Structural Permeability Assessment Using Geological Structural Model Integrated with 3D Geomechanical Study and Discrete Facture Network Model in Wayang Windu Geothermal Field, West Java, Indonesia. In Proceedings 40th Workshop of Geothermal Reservoir Engineering, Stanford, California.

Meyer, B. R., & Bazan, L. W. (2011, January). A discrete fracture network model for hydraulically induced fractures-theory, parametric and case studies. In SPE hydraulic fracturing technology conference. Society of Petroleum Engineers.

Meyer, B.R. MFRAC user's guide, 2016.

Meyer, B.R. Design Formulae for 2-D and 3-D Vertical Hydraulic Fractures: Model Comparison and Parametric Studies, SPE-15240-MS, Louisville, 1986.

Meyer, J.J. et al., Understanding the causation of shear induced casing failure: potential application to induced seismicity, GeoConvention Calgary, 2017

Mikhailov, D. N., Economides, M. J., & Nikolaevskiy, V. N. (2011). Fluid leakoff determines hydraulic fracture dimensions: Approximate solution for non-Newtonian fracturing fluid. International Journal of Engineering Science, 49(9), 809-822.

Nolte, K. G., & Smith, M. B. (1981). Interpretation of fracturing pressures. Journal of Petroleum Technology, 33(09), 1767-1775.

Perkins, T. K., & Kern, L. R. (1961). Widths of hydraulic fractures. Journal of Petroleum Technology, 13(09), 937-949.

Rachmat, S., Asri, M., Treatment Design of Hydraulic Fracturing and Economic Analysis on Water Dominated Geothermal Field. Proceedings 41th Workshop on Geothermal Reservoir Engineering, Stanford, 2016.

Roodhart, L. P., Fokker, P. A., Davies, D. R., Shlyapobersky, J., & Wong, G. K. (1994). Frac-and-pack stimulation: Application, design, and field experience. JPT, Journal of Petroleum Technology;(United States), 46(3).

Rutqvist, J., Tsang, C. F., & Tsang, Y. (2004). Analysis of stress and moisture induced changes in fractured rock permeability at the Yucca mountain drift scale test. In Elsevier Geo-Engineering Book Series (Vol. 2, pp. 161-166). Elsevier.

Salim, P., & Amani, M. (2013). Principal Points in Cementing Geothermal Wells. Advances in Petroleum Exploration and Development, 5(1), 77-91.

ter Heege, J.H., Inventory of quantified risk and impacts of shale gas exploration and exploitation, M4ShaleGas, D21.3, http://www.m4shalegas.eu/, 2017.

Valkó, P., & Economides, M. J. (1999). Fluid-Leakoff Delineation in High-Permeability Fracturing. SPE Production & Facilities, 14(02), 110-116.

Weijers, L., Griffin, L. G., Sugiyama, H., Shimamoto, T., Takada, S., Chong, K. K., ... & Wright, C. A. (2002, January). Hydraulic fracturing in a deep, naturally fractured volcanic rock in Japan-design considerations and execution results. In SPE Asia Pacific Oil and Gas Conference and Exhibition. Society of Petroleum Engineers.

Weng, D., Lei, Q., Ding, Y., Wang, Z., Yang, Z., Wu, J., & Huang, J. (2011, January 1). Case Study: Massive hydraulic fracturing in volcanic gas, China. Society of Petroleum Engineers. doi:10.2118/141543-MS

Witherspoon, P. A., Wang, J. S., Iwai, K., & Gale, J. E. (1980). Validity of cubic law for fluid flow in a deformable rock fracture. Water resources research, 16(6), 1016-1024.

Yew, C. H., & Weng, X., Mechanics of Hydraulic Fracturing, 2nd Edition, Elsevier, ISBN 978-0-12-420003-6, 2015.